Statistical Analysis and Diagnosis Methodology for RF Circuits in LCP Substrates

Souvik Mukherjee, *Student Member, IEEE*, Madhavan Swaminathan, *Senior Member, IEEE*, and Erdem Matoglu

***Abstract*—This paper presents the application of a fast and accurate layout-level statistical analysis methodology for the diagnosis of RF circuit layouts with embedded passives in liquid crystalline polymer substrates. The approach is based on layout-segmentation, lumped-element modeling, sensitivity analysis, and extraction of probability density function using convolution methods. The statistical analyses were utilized as a diagnosis tool to estimate distributed design parameter variations and yield of RF circuit layouts for a given measured performance. The results of statistical analysis and diagnosis were compared with measurement results of fabricated filters. Statistical methods were also applied for design space exploration to improve system performance, as well as estimation of yield and diagnosis of faults during batch fabrication.**

***Index Terms*—Bandpass filter, liquid crystalline polymer (LCP), parametric yield, RF synthesis, statistical diagnosis.**

I. Introduction

THE DESIGN of wireless circuits for RF frequencies require precise values of passive components, which is often not satisfied due to manufacturing variations, resulting in yield loss. To alleviate this problem, performance and yield figures for emerging technologies need to be analyzed during the design phase. Fault detection and diagnosis for RF circuits after manufacturing is a time-consuming step in the design cycle. This is because multiple simulations of electromagnetic (EM) structures are required by varying different layout parameters for correlation with the measured response. The focus of this paper is the application of statistical methods that enable fast and accurate diagnosis of batch fabricated RF circuit layouts for new technologies, which significantly reduces the design and fabrication cycle time.

In RF designs, the physical effects of layout, such as EM coupling and parasitics, affect circuit performance. Though statistical analyses of RF circuits that are based on circuit simulators are fast, they do not provide accurate results. The conventional method to study the effect of component variations on system performance is to perform Monte Carlo analysis [1]. However, Monte Carlo technique for EM simulations can be time and memory intensive. In addition, Monte Carlo analyses do not provide diagnosis capability. The simulation time, in general, for a method of moments (MoM)-based iterative solver increases as $O(n^2)$, where n is the number of cells in the layout. Hence, EM simulation of statistical variations in layout, which requires small cell sizes, makes it memory intensive. Classical worst case analysis in this case is limited since it involves a large number of input–output parameters and impractical simulation time [2]. Clearly there is a need for time-efficient layout-level diagnosis of RF circuits in prototype designs, as well as in volume production based on batch fabrication methods.

Fig. 1. Batch-fabricated bandpass filters on a single panel; each block represents a filter.

Large-area $(12\text{ in} \times 18\text{ in})$ processing, which enables batch fabrication of devices using embedded passives in LCP substrate, is a new technology being developed [3]–[5]. The process enables the manufacturing of 2000–10 000 devices on a single panel, as shown in Fig. 1. In batch fabrication of devices (e.g., bandpass filters), different devices can have different shifts in frequency/phase response characteristics (e.g., bandwidth, center frequency, return loss, etc.). A robust method that captures both forward and reverse mapping of layout parameters to electrical specifications have been applied to synthesis and diagnosis of prototype designs by the same authors in [6]. This paper extends the study on discrete diagnosis to discuss statistical methods that can be utilized to diagnose batch-fabricated designs with reduced EM simulation time. The results of statistical analysis have been compared with EM modeling and measurement data.

A statistical design centering approach to minimax circuit design has been presented in [7]. The method focused on yield optimization based on *circuit level* parameters rather than *layout*. Similar studies based on parametric sampling have been shown in [8]. This method permits the incorporation of realistic manufacturing constraints and resorts to a single stage of statistical simulation, thereby improving time and efficiency. However, the method is limited by its initial requirement of a large database, which can be computationally prohibitive for RF designs

Manuscript received April 4, 2005; revised June 14, 2005.

S. Mukherjee and M. Swaminathan are with the Department of Electrical and Computer Engineering, Georgia Institute of Technology, Atlanta, GA 30332 USA (e-mail: souvikm@ece.gatech.edu; madhavan.swaminathan@ece.gatech.edu).

E. Matoglu is with the IBM Corporation, Austin, TX 78758 USA.

Digital Object Identifier 10.1109/TMTT.2005.855735

on emerging technologies. Earlier research on *circuit-level* design centering led to the development of algorithms based on convexity, radial exploration, and local linear models [9]–[11]. Parasitic-aware post-optimization design centering for RF integrated circuits based on simulated annealing [12] reduces iterations in *design optimization*, but this study does not focus on *diagnosis. Network-level* design centering based on constraint region and piecewise ellipsoidal approximation has been shown in [13], [14]. Statistical fault diagnosis using surface response and center of gravity methods has only been shown for analog integrated circuits in [15], [16], where physical effects of *layout* do not affect performance. Diagnosis of *circuit parameters* based on the Huber concept have been shown in [17], but it does not deal with *physical parameters*, which are measured in batch-fabricated devices to detect process faults. Clearly, the focus of most of the prior research has been *design centering* using *circuit parameters* and not *layout-level diagnosis* of RF designs.

In this paper, efficient layout-level statistical analysis and diagnostic methodologies are presented for RF circuits. The diagnosis method has been demonstrated on a multilayered organic substrate with liquid crystalline polymer (LCP) dielectric material ($\varepsilon_r = 2.95$, $\tan\delta = 0.002$), which is a new technology for embedding RF passive devices [3]–[5]. The statistical diagnosis method is based on layout segmentation, fractional factorial array simulation, sensitivity analysis, regression fitting, and use of least squares and convolution methods to obtain probability distributions of process variations and performance measures. Its advantages, apart from its generic nature and computational efficiency are: 1) it computes probability density functions (pdfs) of performance measures from process distributions; 2) it estimates yield from statistical distributions of layout-level parameters, and, most importantly; 3) it enables circuit diagnosis by mapping layout variations to measured performance.

This paper is organized as follows. Section II discusses the concepts and steps involved in prototype diagnosis and probabilistic diagnosis of RF circuit layouts. The features of the LCP substrate, which is used as a platform for correlating analysis to measurement results, is explained in Section III. Section IV discusses in detail the steps involved in statistical analysis and probabilistic diagnosis with examples. This paper finally concludes with a summary of the contributions of this study in Section V.

II. Diagnosis

Diagnosis is the process of detecting faults in circuits after fabrication, which can be used to improve design yields. Fault diagnosis methodologies are prevalent in digital circuits. In RF designs, however, physical effects of layout affect circuit performance. In [6], and in this paper, diagnosis methods have been discussed for two scenarios, which are: 1) discrete diagnosis to be applicable in the design of prototypes and 2) probabilistic diagnosis based on statistical analysis for batch-fabricated designs, respectively.

A. Prototype Diagnosis Based on Synthesis: Concept

Synthesis is the process of extracting network/layout level parameters for a component/circuit from electrical specifications. It is based on layout segmentation, lumped-element modeling, nonlinear mapping using polynomial functions, and circuit level optimization, as shown in [3]. In [6], the authors have applied the synthesis-based technique to the diagnosis of prototype designs. The variations in measurement data from EM simulation were applied to the synthesis flow to extract new layout geometries, which are different from the origin layout parameters. The result is nonunique since multiple combinations of layout variation give the same shift in frequency response characteristics. Certain designs met the process constraints and were selected for a cross-sectional analysis by which faulty designs could be detected. A detailed mathematical formulation of a synthesis-based prototype diagnosis can be found in [6].

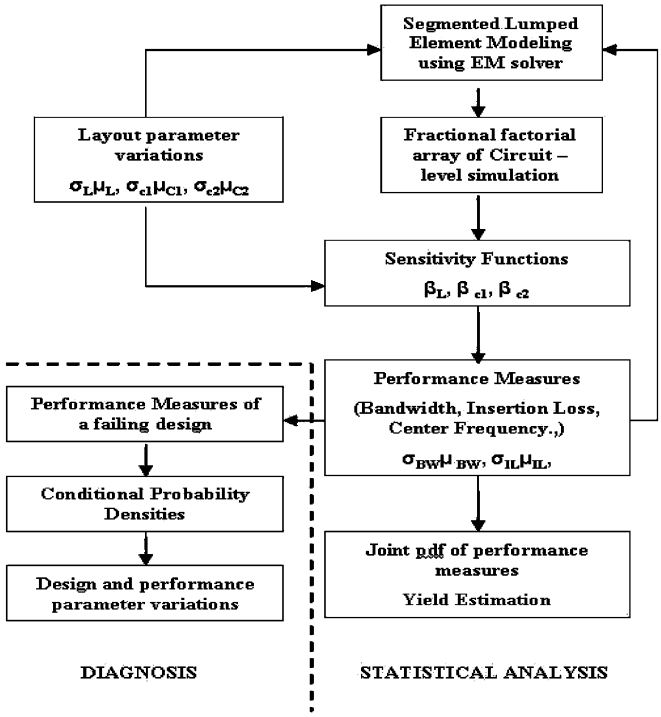

Fig. 2. Block diagram of the statistical analysis and diagnosis methodology.

B. Probabilistic Diagnosis Based on Statistical Analysis: Concept

Fig. 2 shows the flow diagram of the proposed statistical analysis and diagnosis method discussed in this paper. The process begins by identifying key performance measures and significant design parameters. After constructing an accurate model of the system, performance measures were approximated as sensitivity functions of the design parameters through circuit and EM simulations. In these simulations, the design parameters were varied only within their statistical variation ranges to improve accuracy and simulation data size.

Linear and pwl regression equations can be used to map multiple performance measures to physical parameters. Although the methods were not very suitable for obtaining response functions over wide ranges of parameters, they can be used for fast characterization in *small* (<5%) statistical variation "space," which is the case for diagnosis. Yield and performance analysis can be performed after computing the joint probability distribution function (jpdf) of the analyzed performance measures.

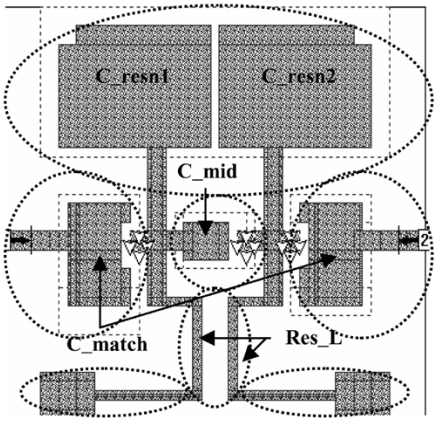

Fig. 3. Layout of the bandpass filter in SONNET.

Parametric causes of the unacceptable performance of an individual system can then be searched by using the information acquired from the statistical analysis, thereby performing layout-level diagnosis. Instead of function failures, this paper focuses on parametric failures, which occur due to the statistical variation in design and performance parameters.

III. Embedded Passives in LCP Substrate

LCP is a low-loss material $(\tan\delta = 0.002)$ with a relative permittivity (ε_r) of 2.95. These properties are invariant up to 100 GHz with negligible moisture absorption (0.04%). As a result, the embedded passives provide high-Q and stable component values across a large frequency range [4]. The process is low cost due to the use of large area manufacturing, as shown in Fig. 1. Furthermore, the process is low temperature (200 °C) and large area boards $(12\text{ in} \times 18\text{ in})$ can be batch fabricated, making it compatible with a printed wiring board (PWB) infrastructure. High-performance and miniaturized filters, low-noise amplifiers, and voltage-controlled oscillators functional from 500 MHz to 10 GHz using embedded inductors and capacitors in multilayer organic laminate substrate such as LCP have been shown in [3]–[5]. The design cross section has two inner metal layers for passives embedded in LCP (1-mil thick) in the middle of the cross section. In addition, top and bottom ground planes are 73 mil from each other and provide EM shielding.

IV. Probabilistic Diagnosis Based on Statistical Analysis

A. Segmented Lumped-Element Modeling and Simulation

Segmented lumped-element modeling of circuits had been explained in [3] and [6] by Mukherjee *et al.* Fig. 3 shows the segmentation of a layout of a bandpass filter into multiple sections. The lumped-element models of these sections have been shown in [6], and are combined to extract the filter performance measures in the circuit simulator. The segmented components were simulated in SONNET, a two-and-one-half-dimensional (2.5-D) MoM-based EM solver in order to extract their model parameters. This is because simulation of the whole filter in an EM solver is computationally expensive. In order to map process variations to performance metrics, EM simulations were planned using design of experiments (DoE) principles, which is common in statistical data analysis [18], [19].

TABLE I
Showing Simulation Matrix Setup

Experiment	A	B	C	D=AB²C²
1	0	0	0	0
2	1	0	0	1
3	2	0	0	2
4	0	1	0	2
5	1	1	0	0
6	2	1	0	1
7	0	2	0	1
8	1	2	0	2
9	2	2	0	0
10	0	0	1	2
11	1	0	1	0
12	2	0	1	1
13	0	1	1	1
14	1	1	1	2
15	2	1	1	0
16	0	2	1	0
17	1	2	1	1
18	2	2	1	2
19	0	0	2	1
20	1	0	2	2
21	2	0	2	0
22	0	1	2	0
23	1	1	2	1
24	2	1	2	2
25	0	2	2	2
26	1	2	2	0
27	2	2	2	1

In this paper, design parameters were varied only within their statistical variation ranges. Therefore, third-order and higher order effects were ignored. Equation (1) shows the quadratic model for n design parameters as follows:

$$y = \beta_0 + \sum_{i=1}^{n} \beta_i x_i + \sum_{i=1}^{n}\sum_{j=1}^{n} \beta_{ij} x_i x_j + \varepsilon \qquad (1)$$

where y is the approximated response, x's are design parameters, β_o is the intercept term, β_i's are coefficients of first-order effects, β_{ij} are coefficients of second-order effects, and ε is the approximation error. If $i \neq j$, β_{ij} is called the interaction coefficient. One way to plan the experiments is to simulate all combinations of the design factors at all levels. This is called the full-factorial experimentation. If m is the level of the experiment plan and n is the number of design parameters, full-factorial experiment results in m^n simulations, which can be prohibitively time consuming for full-wave EM simulations in RF circuits. The number of simulations in the fractional factorial experiment plan is defined as m^{n-p}, where p is the fraction element. For example, 3^{4-1} plan simulates four factors in 27 simulations. The plan is 1/3 fraction of 3^4 full factorial plan. Table I shows a 3^{4-1} array, where 0's, 1's, and 2's correspond to different levels of factors A–D. The elements of the simulation matrix were coded values of the manufacturing variations, where 1's represent their mean, 0 and 2 are $\mu - 3\sigma$ $\mu + 3\sigma$, respectively, where μ is the mean, and σ is the standard deviation. The component values in the table were obtained from SONNET EM simulations. Using the component values in each row, ADS circuit simulations were performed to obtain the filter performance. A second table was

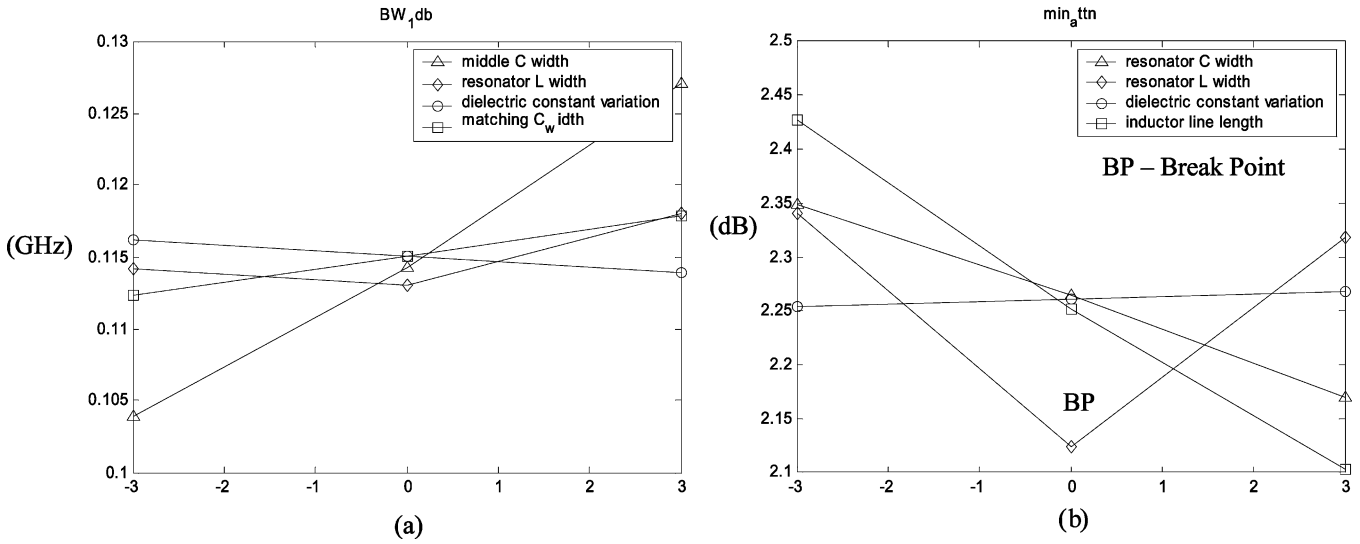

Fig. 4. (a) and (b) Sensitivity plots for filter performance measures against layout parameters. The layout parameters has been converted to standard normal by $(x-\mu_x)/\sigma_x$, as shown by the x-axis. (a) Depicts sensitivity for 1-dB bandwidth. (b) Depicts sensitivity for in-band attenuation (insertion loss).

generated with the results for the filter performance measures. Each row represented a different simulation condition. The filter performance was, therefore, related to layout parameters.

B. Sensitivity Analysis

The effects of the parameters could be plotted by averaging the response at each level. As an example, Fig. 4(a) and (b) shows the sensitivities of certain performance measures with respect to layout parameters, the slopes being the measure of sensitivity. For example, C_mid (Fig. 3) is important for bandwidth, while C_resn1/Res_L (Fig. 3) is important for insertion loss (min_attn). Based on the linearity and piecewise linearity of the plots, performance measures can be represented as first-order linear approximations. For example, a performance measure P^i can be linearly approximated as a regression equation [20] as

$$P^i = \beta_{i0} + \beta_{i1}X^1 + \beta_{i2}X^2 + \cdots + \beta_{\text{in}}X^n + \varepsilon_i \qquad (2)$$

where n is the number of layout parameters, β's are the sensitivity coefficients, and X^i's are the layout parameters converted to the standard normal by $(x-\mu_x)/\sigma_x$. Regression errors are given by ε_i. For example, the sensitivity equations for the filter in Fig. 3 for 1-dB bandwidth (BW_1dB), and attenuation at 2.1 GHz (attn_2_1_GHz) against layout parameters like width of center capacitor (C_mid), width of resonator capacitor (C_resn1/2), width of resonator inductor (Res_L), matching capacitor width (C_match), and dielectric constant of substrate (ε_r) have been shown in (3) and (4) as follows:

$$\begin{aligned}\text{BW\_1dB} = {} & 0.1131 - 0.0426(\text{C\_mid}) \\ & + 0.0023(\text{C\_resn1}) \\ & + 0.0020(\text{Resn\_L})\text{U}(\text{Resn\_L}) \\ & - 0.004(\varepsilon_r) \quad (R^2 = 0.995) \qquad (3)\\ \text{attn\_2\_1\_GHz} = {} & 31.6096 + 1.3361(\text{Resn\_L}) \\ & + 0.2644(\text{C\_resn1}) - 0.3356(\varepsilon_r) \\ & + 2.9389(\text{C\_match}) \quad (R^2 = 0.975). \qquad (4)\end{aligned}$$

Here, R^2 represents regression coefficients, a measure of model fitness [19], and U is the unit step function. R^2 values close to 1 indicate good predictive capability of approximation equations. The simulation matrix was a resolution four $L_{27}(3^4)$ fractional factorial plan [18]. The $L_{27}(3^4)$ matrix does not confound single factor effects into two factor interactions. In order to show that interaction effects are negligible, simulation plan and the filter performance were applied to the response surface regression (RSREG) procedure in SAS software.[1] It was seen that the R^2 values of the cross products (e.g., 0.0007, 0.0021, 0.0005, and 0.0005) were very small compared to the corresponding R^2 values of the linear terms (e.g., 0.7052, 0.8892, 0.9977, 0.9978). For min_attn, ripple, BW_1 dB, and BW_3 dB, the R^2 values of the quadratic effects are significant, therefore, these performance measures were approximated by piecewise linear (pwl) equations, the variables being insertion loss, ripple, 1-dB, and 3-dB bandwidths, respectively. The sensitivity coefficients were obtained with least square approximation, as discussed in [21]. For example, the coefficients for BW_1 dB and attn_2_1_GHz were obtained as follows:

$$[\beta_{\text{BW\_1dB}}] = \left([E]^T[E]\right)^{-1}[E]^T[\text{bW\_1dB}] \qquad (5)$$

$$[\beta_{\text{attn\_2\_1\_GHz}}] = \left([E]^T[E]\right)^{-1}[E]^T[\text{attn\_2\_1\_GHz}] \qquad (6)$$

where E is the simulation matrix (explained in Section IV-A), while [BW_1dB] and [attn_2_1_GHz] are the simulation results from the table generated using DOE. In (5) and (6), the approximation error ε^i for the performance measure P^i can be calculated as follows:

$$\left[\varepsilon^i\right]_{27X1} = P^i - [E]\left(\left([E]^T[E]\right)^{-1}[E]^T\right)\left[P^i\right]. \qquad (7)$$

C. Extraction of pdfs of Performance Measures

Using the regression equations of the performance measures and the pdfs of the layout variations, the pdfs of the performance measures can be computed. The statistical variations of

[1]SAS Software, ver. 8, SAS Inst., Detroit, MI, 1999.

the layout parameters of components are independent of each other. This provides a significant advantage in computing the filter performance based on their variations. In general, let y be a random variable defined as

$$y = y_0 + h_1(x_1) + h_2(x_2) + h_3(x_3) + \cdots + h_n(x_n) \quad (8)$$

where $h_1, h_2, \ldots h_n$ are functions of the independent random variables $x_1, x_2, \ldots x_n$. Then the pdf of y is defined as [18]

$$f_y(y) = \delta(y - y_0) \otimes f_{h1}\big(h_1(x_1)\big) \otimes f_{h2}(h_2(x_2)) \otimes \cdots\cdots \otimes f_{hn}\big(h_n(x_n)\big) \quad (9)$$

where δ is the delta function, $\otimes$ is the convolution operator, and $f_{h1}(h_1(x_1)), \ldots, f_{hn}(h_n(x_n))$ are the pdfs of $h_1(x_1), \ldots, h_n(x_n)$. Given the pdf of a random variable x_k, $f_{xk}(x_k)$ and a function $h_k(x_k)$, the pdf of the random variable h_k can be computed as [19]

$$f_{hk}(h_k) = \frac{f_{xk}(x_{k1})}{\left|\dot{h}_k(x_{k1})\right|} + \frac{f_{xk}(x_{k2})}{\left|\dot{h}_k(x_{k2})\right|} + \cdots + \frac{f_{xk}(x_{kn})}{\left|\dot{h}_k(x_{kn})\right|} \quad (10)$$

where $x_{k1}, x_{k2}, \ldots, x_{kn}$ are solutions to the equation $h_k - h_k(x_k) = 0$ for a specific value of h_k, and $\dot{h}_k$ is the derivative of h_k. For cases in (3) and (4), $h_k(x_k) = \beta_k(x_k)$, where β_k is the coefficient from the regression equation. We then have [18]

$$f_{hk}(h_k) = \frac{f_{xk}\left(\dfrac{h_k}{\beta_k}\right)}{|\beta_k|}. \quad (11)$$

Therefore, the pdfs of the performance measures can be computed by convolving the pdfs of the summation terms in (3) and (4), as follows:

$$f_{P^i}(P^i) = \delta\left(P^i - \beta_{i0}\right) \otimes f(\beta_{i1}X1) \otimes f(\beta_{i2}X2) \otimes \cdots\cdots \otimes f(\beta_{\text{in}}Xn). \quad (12)$$

It can be seen that some of the sensitivity plots in Fig. 4(a) and (b) are pwl. A pwl relation between a variable x and a parameter y can be written as follows:

$$y = \beta_0 + \beta_1 x + \beta_2(x - \text{BP})U(x - \text{BP}) + \varepsilon \quad (13)$$

where $\beta_{0,1,2}$ are regression coefficients, BP is the breakpoint, ε is the regression error, and U is the unit step function defined as $U(x) = 1$ if $x \geq 0$ and $U(x) = 0$ otherwise. Equation (13) can be rewritten as

$$y = \left\{ \begin{array}{ll} \beta_0 + \beta_1 x + \varepsilon, & \text{if } x < BP \\ (\beta_0 - \beta_2 BP) + (\beta_1 + \beta_2)x + \varepsilon, & \text{if } x \geq BP \end{array} \right\}. \quad (14)$$

The coefficients β_0, β_1, and β_2 in (13) were obtained by the least square approximation of y with the parameters x and $xU(x - BP)$ [20]. The pdf of the performance measure with linear and pwl terms can be written as an example for P^i as follows:

$$f_{P^i}(P^i) = \delta\left(P^i - \beta_{i0}\right) \otimes f(\beta_{i1}X1) \otimes f\big(\beta_{i2a}X2 \otimes \beta_{i2b}X2U(X2)\big) \otimes \cdots \otimes f(\beta_{\text{in}}Xn). \quad (15)$$

TABLE II
SHOWING STATISTICAL PARAMETERS OF FILTER PERFORMANCE (FIG. 3)

Filter performance	Mean(μ)	Standard Deviation(σ)
Min_attn (dB)	2.1714	0.0743
Ripple (dB)	0.4894	0.0613
f1(GHz)	2.3525	0.0437
f2(GHz)	2.4271	0.0474
BW_1dB(GHz)	0.1139	0.0041
BW_3B(GHz)	0.135	0.0065

Here, $X2$ was a pwl term. In order to compute the individual functions of (14), (15) can be used to compute the pdf of the terms multiplied with linear coefficients. The pdf of pwl terms in (15), in general, for positive and negative β's is derived in [19]. Since $f_x(x)$ is normally distributed with $\mu = 0$ and $\sigma = 1$, $(f_x(y/\beta))/|\beta|$ is the normal distribution of y with $\mu = 0$ and $\sigma = \beta$. Therefore, for the pwl terms $y = \beta_1 x + \beta_2 xU(x)$, the pdf of y can be computed as

$$f(y) = N\big(y, 0, |\beta_1|\big)U\left(\frac{y}{(-\beta_1)}\right) + N\big(y, 0, |\beta_1 + \beta_2|\big) \times U\left(\frac{y}{(\beta_1 + \beta_2)}\right) \quad (16)$$

where $N(r, \mu, \sigma)$ is the normal pdf of random variable r with mean (μ) and standard deviation (σ). For first-order linear approximated performance measures, the μ and σ values were computed as follows:

$$\mu = \beta_0 \text{ and } \sigma = \sqrt{\sum_{i=1}^{k} \beta_i^2 \sigma_{x_i}^2}. \quad (17)$$

For pwl approximated performance measures, μ and σ values were computed as follows:

$$\mu = \beta_o + \sum_{i=1}^{n} \frac{\beta_{i2}}{\sqrt{2\Pi}} \quad (18a)$$

$$\sigma = \sum_{i=1}^{n} \sqrt{\frac{(\beta_{i1} + \beta_{i2})^2}{2} + \frac{(\beta_{i1})^2}{2} - \frac{(\beta_{i2})^2}{2\Pi}} \quad (18b)$$

where β_{i1} and β_{i2} are the coefficients of x_i and $x_i U(x_i)$ terms. The calculated statistical parameters for the performance measures have been tabulated in Table II. Fig. 5 shows the pdf for the minimum attenuation using convolution.

Fig. 6 shows the histogram for the minimum attenuation. In Fig. 5, the solid line is the convolution, while the dotted line gives the normal distribution, which displayed good agreement with the convolution results. The convolution results have also been compared to the histogram of 100 000 random parameter instances applied to (15) for corresponding performance measures. The convolution results were multiplied by a constant for visual comparison with the histogram. Fig. 6 shows the results. Close agreement was observed between the convolution and the histogram, indicating that the convolution result represents the actual probability density. Skewness and kurtosis are measures of departure from normal distribution. They are defined as (μ^3/σ^3) and (μ^4/σ^4), respectively, where μ^3 and μ^4

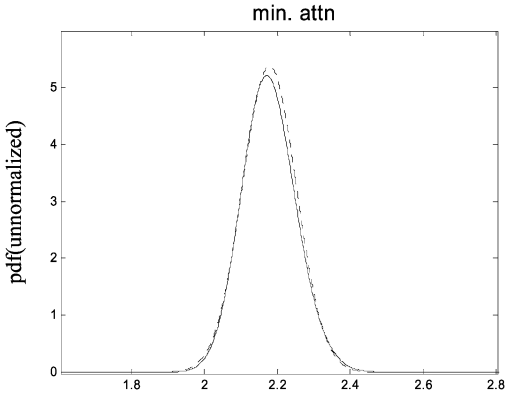

Fig. 5. Comparison of pdfs (y-axis) for insertion loss (min_attn) using convolution (solid line) and normal approximation (dotted line). x-axis depicts the distribution of insertion loss.

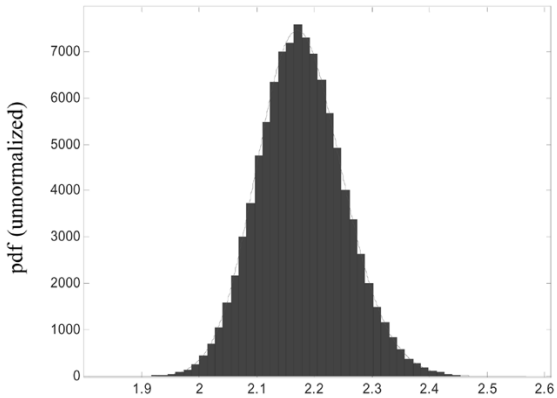

Fig. 6. Comparison of pdfs (y-axis) for insertion loss (min_attn) using convolution (solid line) and random instances (histogram). x-axis depicts the distribution of insertion loss.

are the third and fourth statistical moments and σ is the standard deviation. Clearly, the skewness and kurtosis for normal distribution are 0 and 3, respectively. For the random samples in Fig. 6, skewness and kurtosis were computed as 0.1786 and 3.1112, indicating that they are distributed very close to normal. Similar analysis on the 3-dB bandwidth (BW_3dB) resulted in skewness of 0.0086 and kurtosis of 3.0146.

D. Parametric Yield

Parametric yield is defined as the percentage of the functional filters satisfying the performance specifications. Here, multiple constraints need to be met, e.g., bandwidth, ripple, and center frequency. However, due to the manufacturing variations, certain parameters get shifted in the frequency/amplitude spectrum. In such cases, the jpdfs of the performance measures was approximated using multivariate normal distribution [18], which is defined as follows:

$$f_Y(Y) = \frac{\exp\left\{\frac{-1}{2}\left([Y]-\mu_Y\right)^T\left[\mathrm{Cov}(Y,Y)\right]^{-1}\left([Y]-\mu_Y\right)\right\}}{(2\pi)^2\left|\mathrm{Cov}(Y,Y)\right|^{1/2}} \tag{19}$$

where Y is the vector of performance measures, and μ_Y is the expected value for the vector Y. As an example, the Y vector and μ_Y vector are defined as

$$Y = \begin{bmatrix} f\_1\mathrm{dB}\_1 \\ f\_1\mathrm{dB}\_2 \\ \min\_\mathrm{attn} \\ \mathrm{attn}\_2\_1\mathrm{GHz} \end{bmatrix} \quad \mu_Y = \begin{bmatrix} 2.3348\ (\mathrm{GHz}) \\ 2.4499\ (\mathrm{GHz}) \\ 2.1714\ (\mathrm{dB}) \\ 31.6096\ (\mathrm{dB}) \end{bmatrix}. \tag{20}$$

Covariance of performance measures was computed as [2]

$$\mathrm{Cov}(y_m, y_n) = \sum_{i=1}^{4}\sum_{i=1}^{4}\left(\frac{(\beta_{m-ia}\beta_{n-ka})}{2} + \frac{(\beta_{m-ia}+\beta_{m-ib})(\beta_{n-ka}+\beta_{n-kb})}{2} - \frac{(\beta_{m-ia}\beta_{n-ka})}{2\pi}\right)\delta(i-k) \tag{21}$$

where β_{m-ia}, β_{m-ib} and β_{n-ka}, β_{n-kb} are pwl coefficients of filter performance measures y_m and y_n, respectively, and $\delta(i-k)$ is the impulse function. For the manufacturing parameters with linear sensitivity relations, $\beta_{m-ib} = 0$ and $\beta_{n-kb} = 0$. The yield was then computed as the integral of (19) over the acceptable region of performance. The yield constraints of a filter design were 1-dB bandwidth cutoff frequencies f_1dB_1 and f_1dB_2, min_attn and attn_2_1GHz, the attenuation at 2.1 GHz. The constraints included bandwidth of at least 2.35–2.45 GHz, maximum attenuation of 2.8 dB and minimum attenuation of 30 dB at 2.1 GHz. The yield is calculated as follows:

$$\int_{-\infty}^{2.35}\int_{2.45}^{\infty}\int_{-\infty}^{2.8}\int_{30}^{\infty} f_Y(Y)\,d_{f\_1\mathrm{dB}\_1}\,d_{f\_1\mathrm{dB}\_2} \times d_{\min\_\mathrm{attn}}\,d_{\mathrm{attn}\_2\_1\mathrm{GHz}} = 15.7\%. \tag{22}$$

Further, using the joint probability distribution of performance measures and computing the acceptability function, it can be inferred whether simultaneous constraints on a pair of performance measures is physical or not. This has been shown in Figs. 7 and 8. In these figures, the acceptability function (z-axis) has not been normalized. From Fig. 7, it can be seen by just the two spikes (indicating design acceptability) that simultaneous constraints on the attenuation at 2.1 GHz and the lower side frequency of the 1-dB bandwidth leads to a nonphysical result. This means that certain design constraints cannot be met simultaneously and will result in very low yield. On the other hand, the distribution of the acceptability function in Fig. 8 indicates that it is reasonable to place simultaneous constraints on in-band ripple and lower side frequency of the 1-dB bandwidth. For example, the theoretical yield of the bandpass filter design increased from 25.7% to 35% when simultaneous constraints were changed from {in-band ripple, lower side 1-dB frequency} to {1-dB bandwidth, in-band ripple}. This suggests that the yield of a design can be improved by identifying the parameters on which to place design constraints simultaneously. Here, acceptability function implies whether a device has met the design criteria. The function is positive when they are met.

Further, it is clear that the yield of the bandpass filter can be improved by reducing the manufacturing variations. If the

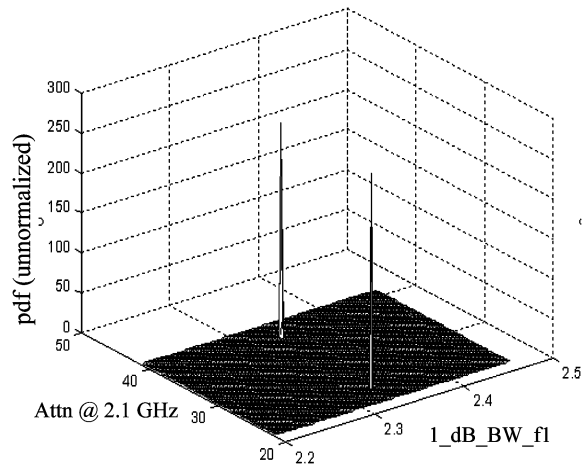

Fig. 7. Distribution of design acceptability function using simultaneous constraints on attenuation @2.1 GHz and lower cutoff frequency of 1-dB bandwidth: isolated spikes indicate that such constraints lead to low yield.

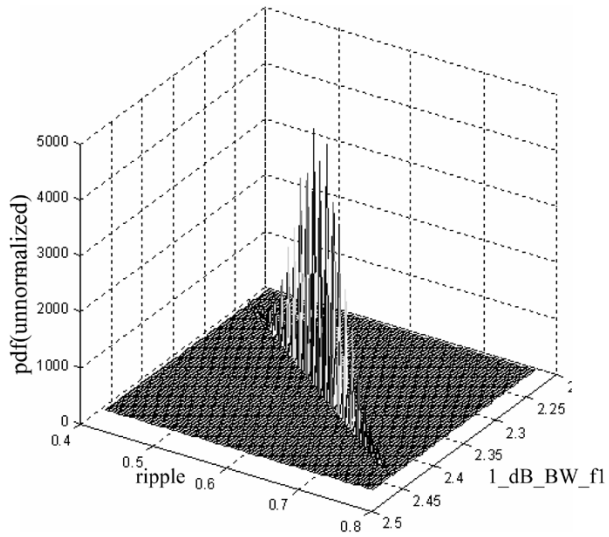

Fig. 8. Computation of design acceptability function using simultaneous constraints on in-band ripple and lower cutoff frequency of 1-dB bandwidth: distribution shows that such constraints lead to realizable yield.

standard deviation (σ) of the all physical parameters could be reduced to $\sigma/2$, reevaluation of the integral in (22) results in a yield of 31.5%. Further reduction of σ to $\sigma/4$ results in a 43.8% yield. It was also observed that the yield does not increase unless additional performance tolerance was provided. As an example, with an additional increase of $2\Delta\mathrm{BW} = 10$ MHz in the 1-dB bandwidth, the yield increased to 20%. Using figures of joint distributions and yield variations with design tolerance, yield targets can be achieved by the most feasible design and manufacturing changes.

E. Diagnosis Based on Statistical Analysis

As a result of the statistical variations in design and operational parameters in batch fabrication, some circuits display unacceptable variations in performance measures. For a functional design in this condition, the information extracted from the aforementioned statistical analysis can be utilized as a diagnosis tool. Using the diagnosis methodology, the most probable layout parameters causing the unacceptable variations in performance measures can be systematically searched. For example, the linear systems formed by (3) and (4) can be used to estimate the variation in the design and operational parameters for the measured variations in system performance. Here, the analysis can be broken into two sections. When the number of performance measures in a design is *less* than the number of layout parameters, it suggests infinite number of solutions and, therefore, a probabilistic approach is used, as is explained in Section I. When the number of performance measures is *more* than the number of physical parameters, it suggests a solution of linearly independent equations (Section II).

1) Number of Performance Measures Less Than Number of Physical Parameters $(n < m)$: For explaining the diagnosis approach, let $[X]$ and $[Y]$ be the random vectors for m layout parameters and n performance measures, respectively. The functional relation between $[X]$ and $[Y]$ $(R^m \rightarrow R^n)$ was obtained by characterization simulations explained above. If n is less than m, then a unique solution of $[X]$ does not exist for a measured set of unacceptable performance $[Y]$. Hence, the real parameter(s) causing the failure cannot be decided. However, since all design parameters are associated with pdfs, the most probable solution can be searched. The conditional pdf of the parameter vector $[X]$ for measured performance y is defined as [19]

$$f(X \mid Y = y) = \frac{f(X,Y)}{f(Y)} \tag{23}$$

where $f(X,Y)$ is the jpdf of the random vector of the design parameters and performance measures $[X^T Y^T]^T$. In (23), $f(Y)$ is the jpdf of the performance measures, which was computed in (19). The expected value of $f(X \mid Y = y)$ is then the most probable parameter set causing the failure.

Let $\hat{Y} = [P^1 \quad P^2 \quad \ldots P^n]^T$ be the set of unacceptable performance measures. Equations for the performance measures can be rewritten by subtracting the intercept term $\beta_{10}, \beta_{20}, \beta_{30}, \ldots, \beta_{n0}$ from $\hat{Y}$ resulting in

$$Y = \beta X + \varepsilon \tag{24}$$

where X is the parameter vector and Y and β are defined as the performance vectors $n \times m$ sensitivity coefficient matrix without intercept terms β_{i0}. The error column ε is a Gaussian random vector with a zero mean computed from the approximation errors in error equation. Since X and Y are Gaussian random vectors, a new random vector Z can be defined as $Z_{m\times 1} = [X^T Y^T]^T$. The pdf of Z is then equivalent to the jpdf of X and Y, which can be computed as follows:

$$\begin{aligned} f_Z(Z) &= f_{X,Y}(X,Y) \\ &= \frac{\mathrm{Exp}\left\{-\frac{1}{2}\left([Z]-E[Z]\right)^T \left[\mathrm{Cov}(Z)\right]^{-1}\left([Z]-E[Z]\right)\right\}}{(2\pi)^2 \left|\mathrm{Cov}(Z)\right|^{1/2}} \end{aligned} \tag{25}$$

where $E[Z] = \left[\mu_X^T \; \mu_Y^T\right]^T$, and $\mathrm{Cov}(Z)_{n\times n}$ is a matrix composed of covariance matrices, as shown in [19].

Note that for independent design parameters, $\mathrm{Cov}(X,X)$ is the diagonal matrix of parameter variances. The expected value of the conditional pdf in (23) can be computed as [2]

$$E[X \mid Y=y] = \mu_X + \mathrm{Cov}(X,Y)\big[\mathrm{Cov}(Y,Y)\big]^{-1}(Y-\mu_Y). \tag{26}$$

Since X and Y are related through the linear regression operator defined in (24) as $Y = \beta X + \varepsilon$, then the mean of Y, $\mathrm{Cov}(X,Y)$, and $\mathrm{Cov}(Y,Y)$ are related by relations shown in [21]. The substitution of which results in (27) as follows:

$$E[X \mid Y=y] = \mu_X + \mathrm{Cov}(X,X)\beta^T \times\big[\beta\mathrm{Cov}(X,X)\beta^T + \mathrm{Cov}(\varepsilon)\big]^{-1}(Y-\beta\mu_X). \tag{27}$$

2) Number of Performance Measures More Than Number of Physical Parameters ($n > m$): Let $A_{n\times m}$ be the linear sensitivity matrix that relates n performance measures $Y_{n\times 1}$ to m physical parameters $X_{m\times 1}$ by the following:

$$Y = Y_0 + AX + \varepsilon \tag{28}$$

where Y_0 is a constant vector and ε is the regression error vector. Provided that $(A^TA)^{-1}$ exists, for $n \geq m$, the least square solution was computed as follows [21]:

$$\hat{X} = \big(A^TA\big)^{-1}A^T(Y-Y_0). \tag{29}$$

The sensitivity equations of matrix A, which correspond to its rows, should be linearly independent. Otherwise the (A^TA) matrix is singular and not invertible. If two sensitivity equations in matrix A are linearly dependent, the corresponding performance measures are highly correlated. Therefore, such performance measures should not be included in the sensitivity matrix together. Correlation coefficient takes values between -1 and 1, where large values of $|\rho|$ indicate high correlation. It was observed that many of the performance measures are highly correlated. Therefore, the sensitivity equations are linearly dependent. Amongst linearly dependent equations, only one equation and associated performance measure can be used for diagnosis. In this case, there is infinite number of solutions. Therefore, probabilistic diagnosis outlined in Section IV-E.1 was adopted for the filter. The most probable parameter vector X can be written as

$$\big(X : f\big(X \mid Y=y\big)_{\max}\big) = \mu_X + \mathrm{Cov}(X,Y)\big[\mathrm{Cov}(Y,Y)\big]^{-1}(Y-\mu_Y) \tag{30}$$

where $(X : f(X \mid Y=y)_{\max})$ is the most probable layout parameter vector X for a measured filter performance y, μ_X and μ_Y are the expected values of X and Y, $\mathrm{Cov}(Y,Y)$ is the covariance matrix of the performance measures, and $\mathrm{Cov}(X,Y)$ is the covariance matrix of the layout parameters and the performance measures.

TABLE III
SHOWING ESTIMATED AND MEASURED PARAMETERS

Layout parameter	Meausred parameters	Estimated parameters	Least squares
Resn_L	μ+2.29σ	μ +2.26σ	μ +1.52σ
C_resn	μ -1.34σ	μ -1.66σ	μ -3.95σ
C_mid	μ -0.71σ	μ -0.35σ	μ -6.64σ
C_match	μ +1.92σ	μ +2.27σ	μ +2.76σ

The mean values of the performance measures were presented in Table II. As an example, the Y and μ_Y vector for min_attn, ripple, and $f2$ are defined as follows:

$$Y = \begin{bmatrix} \text{min\_attn} \\ \text{ripple} \\ f2 \end{bmatrix} \quad \mu_Y = \begin{bmatrix} 2.1784\ (\text{dB}) \\ 0.5894\ (\text{dB}) \\ 2.3855\ (\text{GHz}) \end{bmatrix}. \tag{31}$$

The covariance matrix of the performance measures $\mathrm{Cov}(Y,Y)$ was computed using (21). Applying the regression coefficients results in the covariance matrix in (32) as follows:

$$\mathrm{Cov}(Y,Y) = \begin{bmatrix} 0.0055 & -0.0006 & -0.0022 \\ -0.0006 & 0.0038 & 0.0023 \\ -0.0022 & 0.0023 & 0.0021 \end{bmatrix}. \tag{32}$$

The elements of the matrix $\mathrm{Cov}(X,Y)$ is computed as [21]

$$\mathrm{Cov}(x_i, y_n) = \frac{\beta_{n-ia}}{2} + \frac{\beta_{n-ia}+\beta_{n-ib}}{2} \tag{33}$$

where β_{n-ia} and β_{n-ib} are the pwl coefficients of filter performance measure y_n for the layout parameter x_i. For parameters with linear sensitivities, $\beta_{n-ib} = 0$. Using (33), the most probable vector of layout parameters for a measured set of performance can then be computed. Multiple examples illustrate the accuracy of the diagnosis method.

F. Test Cases

1) Bandpass Filter: A bandpass filter with a layout similar to that shown in Fig. 3 and having a 1-dB bandwidth of 115 MHz and a center frequency of 2.38 GHz has been used for statistical analysis in the first example, as explained above. In Table III, as in the first example, a vector of layout parameters with random values was chosen according to their statistical distribution and was modeled and simulated. The resulting performance measures were min_attn $= 1.9933$ dB, ripple $= 0.6513$ dB, and $f2$ (higher side of 1-dB frequency) $= 2.5342$ GHz. For this filter, the center frequency was shifted. The statistical analysis of the performance measures were applied to (30). Table III shows the measured and estimated manufacturing variations in the second and third columns, which show good correlation.

It can be seen that most of the parameters are estimated close to their actual values. The fourth column in this table is the result obtained from the least square solution computed using (29). As explained before, the least square solution can be erroneous due

TABLE IV
SHOWING ESTIMATED AND MEASURED PARAMETERS

Filter performance	Mean(μ)	Standard Deviation(σ)
Min_attn (dB)	1.1714	0.0443
Attn_3_7GHz	40.4894	0.0718
f1(GHz)	2.5213	0.0657
f2(GHz)	3.1871	0.0874
BW_1dB(GHz)	0.4413	0.0056
BW_3B(GHz)	0.6618	0.0065

to the ill-conditioned sensitivity matrix (can be seen from the bad correlation of the parameters).

It is clear that the diagnosis technique do not give the *exact* statistical variation of layout parameters in batch fabrication, but it captures the dominant variations. The results of statistical distributions show good correlation obtained from that using Monte Carlo methods. However, with the extensive EM simulations on layouts and having statistical distributions on all the layout elements, Monte Carlo simulations took 36 h on a Dell PC with 2.6-GHz processor and 1-GB random access memory (RAM).

2) Bandpass Filter With Transmission Zeros: A second example is a filter whose mean and standard deviation for performance measures has been extracted and shown in Table IV. Regression analysis on the fractional factorial array of the design (consisting of 27 simulations) was performed similar to that shown in Example 1.

The pdfs of the performance measures were computed using convolution. The mean and standard deviation has been shown in Table III. Here, Attn_3_7_GHz is the transmission zero location at 3.7 GHz. The parametric yield with constraints on bandwidth, center frequency, and transmission zero was computed using (22) as

$$\int_{3.65}^{3.75}\int_{0.64}^{0.67}\int_{36}^{\infty} f_Y(Y)d_{\text{zero}}d_{\text{BW\_3dB\_2}}d_{\text{CF}} = 35.5\% \quad (34)$$

where zero, BW_3dB, and CF are the transmission zero, 3-dB bandwidth, and center frequency, respectively. The covariance of performance measures was computed using (21) as

$$\text{Cov}(Y,Y) = \begin{bmatrix} 0.0075 & -0.0034 & 0.0049 \\ -0.0034 & 0.0017 & 0.0034 \\ 0.0049 & 0.0034 & -0.0049 \end{bmatrix}. \quad (35)$$

The vector for the performance measures that were selected for diagnosis are given by

$$Y = \begin{bmatrix} \text{attn\_3\_7\_GHz} \\ \text{BW\_3dB} \\ \text{min\_attn} \end{bmatrix} \quad (36a)$$

$$\mu_Y = \begin{bmatrix} 40.4894\,(\text{dB}) \\ 0.6618\,(\text{GHz}) \\ 1.1714\,(\text{dB}) \end{bmatrix}. \quad (36b)$$

TABLE V
SHOWING ESTIMATED AND MEASURED PARAMETERS

Layout parameter	Measured parameters	Estimated parameters
Resn_L	μ -0.25 σ	μ -0.83σ
C_match	μ -2.85σ	μ -3.17σ
C_resn	μ +0.15 σ	μ -0.18σ
C_mid	μ -3.23σ	μ -3.02σ

For diagnosis, the covariance matrix between the performance measures and the physical parameters was calculated as (37), and is given by

$$\text{Cov}(X,Y) = \begin{bmatrix} -0.0458 & 0.0791 & 0.0624 \\ -0.0058 & 0.0325 & 0.0031 \\ 0.0021 & -0.0037 & -0.004 \\ -0.0439 & -0.0035 & 0.0280 \end{bmatrix}. \quad (37)$$

Table V shows the comparison between the observed (measurement) and estimated variation for a randomly selected design on the panel. Clearly, the methodology closely estimates the major variations, which are C_mid width and C_match width compared to measurement results.

V. CONCLUSION

This paper has discussed efficient statistical methodologies for layout-level diagnosis of batch-fabricated RF circuits in LCP substrates. The methodology has demonstrated performance analysis using DOE principles. The techniques has suggested a feasible time-efficient alternative of circuit diagnosis using layout-level parameters with reasonable accuracy compared to time-consuming worst case EM simulations on complete layouts. The methodology could also estimate parametric yield and suggest performance improvement methods. Diagnostic methodologies using statistical analysis could also be used to trace the statistical variations of embedded passive components to performance failure of designs.

REFERENCES

[1] J. M. Hammersley and D. C. Handscomb, *Monte Carlo Methods*. New York: Chapman & Hall, 1983, ch. 4.
[2] S. G. Duvall, "Statistical circuit modeling and optimization," in *Proc. Int. Statistical Metrology Workshop*, Kyoto, Japan, Jun. 2000, pp. 56–63.
[3] S. Mukherjee, B. Mutnury, S. Dalmia, and M. Swaminathan, "Layout-level synthesis of RF inductors and filters in LCP substrates for Wi-Fi applications," *IEEE Trans. Microw. Theory Tech.*, vol. 53, no. 6, pp. 2196–2210, Jun. 2004.
[4] S. Dalmia, G. White, V. Sundaram, and M. Swaminathan, "Liquid crystalline polymer (LCP) based lumped element BPF's for multiple wireless applications," in *IEEE MTT-S Int. Microwave Symp. Dig.*, Fort Worth, TX, Jun. 2004, pp. 1991–1994.
[5] A. Bavisi, S. Dalmia, M. Swaminathan, G. White, and V. Sundaram, "Chip-package co-design of integrated voltage controlled oscillator in LCP substrate," *IEEE Trans. Adv. Packag*, 2005, to be published.
[6] S. Mukherjee, M. Swaminathan, and S. Dalmia, "Synthesis and diagnosis of RF filters in liquid crystalline polymer (LCP) substrate," in *IEEE MTT-S Int. Microwave Symp. Dig.*, Long Beach, CA, Jun. 2005, pp. 456–459.
[7] M. A. Styblinski, "Statistical design centering approach to minimax circuit design," in *Proc. IEEE Int. Circuits and Syst. Symp.*, Portland, OR, May 1989, pp. 697–700.
[8] K. Singhal and J. F. Pinel, "Statistical design centering and tolerancing using parametric sampling," *IEEE Trans. Circuits Syst.*, vol. CAS-28, no. 7, pp. 692–702, Jul. 1981.

[9] S. Sapatnekar, P. M. Vaidya, and S. M. Kang, "Convexity-based algorithms for design centering," *IEEE Trans. Computer-Aided Des. Integr. Circuits Syst.*, vol. 13, no. 12, pp. 1536–1549, Dec. 1994.
[10] K. S. Tahim and R. Spence, "A radial exploration approach to manufacturing yield estimation and design centering," *IEEE Trans. Circuits Syst.*, vol. CAS-26, no. 9, pp. 768–774, Sep. 1979.
[11] M. Li and L. Milor, "Computing parametric yield adaptively using local linear models," in *Proc. IEEE Design Automation Conf.*, Las Vegas, NV, Jun. 1996, pp. 831–835.
[12] K. Choi and D. Allstot, "Post-optimization design centering for RF integrated circuits," in *Proc. IEEE Int. Circuits and Syst. Symp.*, Vancouver, BC, Canada, May 2004, pp. 956–959.
[13] H. L. Malek and A. Hassan, "The ellipsoidal technique for design centering and region approximation," *IEEE Trans. Computer-Aided Des. Integr. Circuits Syst.*, vol. 10, no. 8, pp. 1006–1014, Aug. 1991.
[14] J. Wojciechowski and K. Zamlynski, "Design centering using an approximation to the constraint region," *IEEE Trans. Circuits Syst. I, Reg. Papers*, vol. 51, no. 3, pp. 598–607, Mar. 2004.
[15] J. Gonzalez and G. Verbad, "Fault diagnosis of analog integrated circuits using surface response methods," in *Proc. Int. Statistical Metrology Workshop*, Honolulu, HI, Jun. 1999, pp. 18–21.
[16] M. Keramat and R. Kielbasa, "Optimality aspects of centers of gravity algorithm for statistical circuit design," in *Proc. IEEE Midwest on Circuits Systems Symp.*, Sacramento, CA, Aug. 1997, pp. 95–98.
[17] J. Bandler, S. H. Chen, R. M. Biernacki, and K. Madsen, "The Huber concept in device modeling, circuit diagnosis and design centering," in *Proc. IEEE Int. Circuits and Systems Symp.*, vol. 1, London, U.K., May-Jun. 1994, pp. 129–132.
[18] R. L. Mason, R. F. Gunst, and J. L. Hess, *Statistical Design and Analysis of Experiments: With Applications to Engineering and Science*. New York: Wiley, 1989, ch. 3, 5.
[19] E. Matoglu, "Statistical design, analysis and diagnosis of digital systems and RF circuits," Ph.D. dissertation, School Elect. Computer Eng., Georgia Inst. Technol., Atlanta, 2003.
[20] ——, "Statistical signal integrity analysis and diagnosis methodology for high-speed systems," *IEEE Trans. Adv. Packag.*, vol. 27, no. 4, pp. 611–629, Nov. 2004.
[21] M. H. Kutner, C. J. Nachtscheim, W. Wasserman, and J. Neter, *Applied Linear Statistical Models*. New York: McGraw-Hill, 1996, ch. 2, 6, 7.

Souvik Mukherjee (S'02) received the B.Tech (Hons.) degree in electronics and electrical communication engineering from the Indian Institute of Technology, Kharagpur, India, in 2002, the M.S. degree in electrical engineering from the Georgia Institute of Technology, Atlanta, in 2004, and is currently working toward the Ph.D. degree in electrical engineering at the Georgia Institute of Technology.

In Summer 2005, he interned with Analog Devices Inc. Greensboro, NC, where he was involved with three-dimensional (3-D) EM modeling and simulation of RF front-ends for wireless local area network (WLAN) applications. His research involves modeling, simulation, synthesis and diagnosis of RF passive and active circuits.

Madhavan Swaminathan (A'91–M'95–SM'98) received the M.S. and Ph.D. degrees in electrical engineering from Syracuse University, Syracuse, NY, in 1989 and 1991, respectively.

He is currently a Professor with the School of Electrical and Computer Engineering, Georgia Institute of Technology, Atlanta, and the Deputy Director of the Packaging Research Center, Georgia Institute of Technology. He is the co-founder of Jacket Micro Devices Inc., Atlanta, GA, a company that specializes in integrated devices and modules for wireless applications, for which he serves as the Chief Scientist. Prior to joining the Georgia Institute of Technology, he was with the Advanced Packaging Laboratory, IBM, where he was involved with packaging for super computers. While with IBM, he reached the second invention plateau. He has authored or coauthored over 150 publications in refereed journals and conferences and has coauthored three book chapters. He holds nine issued patents with six pending. His research interests are digital, RF, opto-electronics, and mixed-signal packaging with emphasis on design, modeling, characterization, and test.

Dr. Swaminathan has served as the co-chair for the 1998 and 1999 IEEE Topical Meeting on Electrical Performance of Electronic Packaging (EPEP). He is the co-founder and has served as the technical and general chair for the International Microelectronics and Packaging Society (IMAPS) Next Generation Integrated Circuits (IC) and Package Design Workshop. He serves as the chair of TC-12, the Technical Committee on Electrical Design, Modeling, and Simulation within the IEEE Components, Packaging, and Manufacturing Technology (CPMT) Society and was the co-chair for the 2001 IEEE Future Directions in IC and Package Design Workshop. He is the co-founder of the IEEE Future Directions in IC and Package Design Workshop. He also serves on the Technical Program Committees of the EPEP, Signal Propagation on Interconnects Workshop, Solid-State Devices and Materials Conference (SSDM), Electronic Components and Technology Conference (ECTC), and Interpack. He has been a guest editor for the IEEE TRANSACTIONS ON ADVANCED PACKAGING and the IEEE TRANSACTIONS ON MICROWAVE THEORY AND TECHNIQUES. He was the associate editor of the IEEE TRANSACTIONS ON COMPONENTS AND PACKAGING TECHNOLOGIES. He was the recipient of the 2002 Outstanding Graduate Research Advisor Award presented by the School of Electrical and Computer Engineering, Georgia Institute of Technology and the 2003 Outstanding Faculty Leadership Award for the mentoring of graduate research assistants from the Georgia Institute of Technology. He was also the recipient of the 2003 Presidential Special Recognition Award presented by the IEEE CPMT Society for his leadership of TC-12 and the 2004 IBM Faculty Award. He was the recipient of the Shri. Mukhopadyay Best Paper Award presented at the International Conference on Electromagnetic Interference and Compatibility (INCEMIC), Chennai, India, 2003. He has also served as the coauthor and advisor for numerous outstanding student paper awards at EPEP'00, EPEP'02, EPEP'03, EPEP'04, ECTC'98, and the 1997 IMAPS Education Award.

Erdem Matoglu received the B.S. degree in electrical engineering from Middle East Technical University, Ankara, Turkey, in 1999, and the M.S. degree in electrical engineering and Ph.D. degree from the Georgia Institute of Technology, Atlanta, in 2000 and 2004, respectively.

He joined the Georgia Institute of Technology for graduate studies and became involved in the area of high-speed digital systems modeling in 1999. In 2001, he became involved with statistical analysis of large digital systems. In the summers of 2001 and 2002, he interned with the IBM eServers xSeries group, Austin, TX. His current research interests are in the field of modeling, simulation, and statistical analysis and diagnosis of digital systems.

Dr. Matoglu was the recipient of the Best Student Paper Award presented at the 2002 IEEE Topical Meeting on Electrical Performance of electronic Packaging (EPEP).